Journal of Inorganic and General Chemistry
ZAAC
Zeitschrift für anorganische und allgemeine Chemie

DOI: 10.1002/zaac.201900190

ARTICLE

Mechanochemical Synthesis of $Cu_2MgSn_3S_8$ and $Ag_2MgSn_3S_8$

Eva Maria Heppke,[a] Steffen Klenner,[b] Oliver Janka,[b] Rainer Pöttgen,[b] and Martin Lerch*[a]

Dedicated to Prof. Martin Jansen on the Occasion of his 75th Birthday

Abstract. Two new thiospinels of the type $A^I_2B^{II}C^{IV}_3S^{VI}_8$ were successfully synthesized via a mechanochemical route using binary sulfides and sulfur. $Cu_2MgSn_3S_8$ and $Ag_2MgSn_3S_8$ are the first $A^I_2B^{II}C^{IV}_3S^{VI}_8$ compounds with magnesium as divalent cation. The crystal structures of $Cu_2MgSn_3S_8$ and $Ag_2MgSn_3S_8$ were refined in the cubic space group $Fd\bar{3}m$ using X-ray powder diffraction. According to UV/Vis measurements, a direct optical bandgap of ca. 1.65 eV was determined for both $Cu_2MgSn_3S_8$ and $Ag_2MgSn_3S_8$. Temperature-dependent magnetic susceptibility measurements of the $Cu_2MgSn_3S_8$ sample indicate diamagnetism. A ^{119}Sn Mössbauer spectrum confirms the tetravalent state of tin, underlining the electron-precise description.

Introduction

Some complex Cu- and Ag-based thiospinels with the general formula $A^I_2B^{II}C^{IV}_3S^{VI}_8$ have been described in literature. Most of these compounds are associated with tin such as $Cu_2MSn_3S_8$ with M = Mn, Fe, Co, Ni or $Ag_2MnSn_3S_8$.[1–8] In addition, titanium-containing compounds[9,10] and even one zirconium analogue[11] are hitherto known. The cation-deficient structure of the compounds $A^I_2B^{II}C^{IV}_3S^{VI}_8$ offers the possibility of Li^+ intercalation and therefore these phases are interesting materials for Li-battery cathodes.[2,4,7,12] The compounds $A^I_2B^{II}C^{IV}_3S^{VI}_8$ have been described in the cubic space group $Fd\bar{3}m$[2–4,7,9–12] or the tetragonal space group $I4_1/a$.[1,5] Copper deficiency is also mentioned for this class of materials.[13,14] By mechanochemical milling, two new compounds of the type $A^I_2B^{II}C^{IV}_3S^{VI}_8$ have been successfully synthesized. The main focus of the present study concerns the synthesis, crystal structure, and magnetic behavior of $Cu_2MgSn_3S_8$ and $Ag_2MgSn_3S_8$.

Results and Discussion

Chemical Analysis and Crystal Structure

Two new phase-pure thiospinels, $Cu_2MgSn_3S_8$ and $Ag_2MgSn_3S_8$, were successfully synthesized via a mechanochemical procedure with a subsequent annealing step in H_2S atmosphere. Both compounds crystallize in the cubic space group type $Fd\bar{3}m$ with a = 10.4173(2) and a = 10.6938(2) Å, respectively. The composition of $Cu_2MgSn_3S_8$ / $Ag_2MgSn_3S_8$ was confirmed by energy dispersive X-ray spectroscopy and combustion analysis and is summarized in Table 1. X-ray powder diffraction patterns with the results of the Rietveld refinements are depicted in Figure 1 and Figure 2. Details and refined structural parameters are listed in Table 2, Table 3, and Table 4. The experimental diffraction patterns are in good agreement with the calculated ones, reflected by residual values of R_{wp} = 0.022 for $Cu_2MgSn_3S_8$ and R_{wp} = 0.032 for $Ag_2MgSn_3S_8$. The total occupancies of the cation positions 8*a* and 16*d* were fixed. Wyckoff position 16*d* is occupied statistically by Mg and Sn. Relatively high Debye-Waller factors were obtained for Cu and Ag at position 8*a* (Table 3, Table 4). This has also been observed for monovalent cations in other quaternary thiospinels like $Cu_2CdSn_3S_8$[5] or other crystal structures of quaternary chalcogenides, for example $Ag_2In_2GeSe_6$.[15]

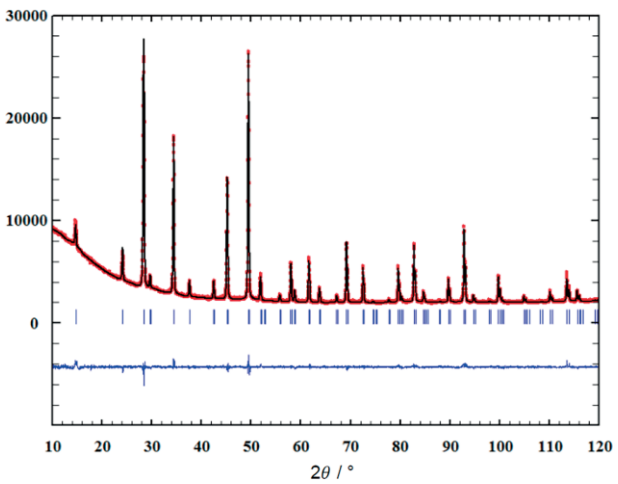

Figure 1. X-ray diffraction pattern of $Cu_2MgSn_3S_8$ with the results of the Rietveld refinement.

* Prof. Dr. M. Lerch
E-Mail: martin.lerch@tu-berlin.de
[a] Institut für Chemie
Technische Universität Berlin
Straße des 17. Juni 135
10623 Berlin, Germany
[b] Institut für Anorganische und Analytische Chemie
Universität Münster
Corrensstraße 30
48149 Münster, Germany

Table 1. Phase composition of $Cu_2MgSn_3S_8$ and $Ag_2MgSn_3S_8$ calculated from EDX and elemental analysis.

$Cu_2MgSn_3S_8$	ideal /at-%	measured /at-%	$Ag_2MgSn_3S_8$	ideal /at-%	measured /at-%
Cu	14.3	15.1	Ag	14.3	14.5
Mg	7.1	6.8	Mg	7.1	7.0
Sn	21.4	24.6	Sn	21.4	22.8
S_{EDX}	57.1	53.9	S_{EDX}	57.1	55.8
S_{EA}	57.1	55.4	S_{EA}	57.1	56.9

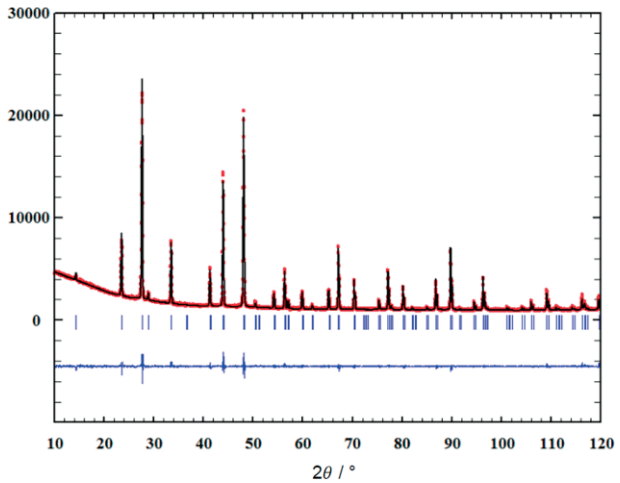

Figure 2. X-ray diffraction pattern of $Ag_2MgSn_3S_8$ with the results of the Rietveld refinement.

Table 2. Results of the Rietveld refinements for $Cu_2MgSn_3S_8$ and $Ag_2MgSn_3S_8$ (standard deviations in parenthesis).

	$Cu_2MgSn_3S_8$	$Ag_2MgSn_3S_8$
Structure type	Spinel	
Space group	$Fd\bar{3}m$	
Crystal system	cubic	
Z	4	
a /Å	10.4173(2)	10.6938(2)
V /Å^3	1130.49(4)	1222.92(4)
Calculated density, g·cm^{-3}	4.49	4.63
Diffractometer	PANalytical X'Pert MDP Pro	
Radiation	Cu-K_α radiation	
Wavelength /Å	λ_1 = 1.54056, λ_2 = 1.54439	
R_p	0.0161	0.0237
R_{wp}	0.0215	0.0324
R_{exp}	0.0175	0.0238
R_{Bragg}	0.0272	0.0212
S	1.23	1.36

As mentioned in the introduction, some $A^I_2B^{II}C^{IV}_3S^{VI}_8$-type phases such as $Cu_2CdSn_3S_8$[5] are reported to crystallize in the tetragonal space group $I4_1/a$. However, structural refinements for $Cu_2MgSn_3S_8$ and $Ag_2MgSn_3S_8$ in lower tetragonal symmetry were also performed but no improvement of the refinement quality has been achieved.

The spinel-type crystal structures of $Cu_2MgSn_3S_8$ and $Ag_2MgSn_3S_8$ are composed of a cubic closest-packed arrangement of sulfide anions. One eighth of the tetrahedral voids is occupied by Cu/Ag which are coordinated by four sulfur anions and form $[CuS_4]^{7-}$ and $[AgS_4]^{7-}$ tetrahedra, respectively. Half of the octahedral voids are filled statistically with Mg and Sn. The Cu-/Ag-centered sulfide tetrahedra share corners with the octahedra which are edge-shared between themselves. The sulfur anion is coordinated by three kinds of atoms including one Cu/Ag and three Mg/Sn with distances varying from 2.3233(10) to 2.5658(10) Å for $Cu_2MgSn_3S_8$ and 2.4825(13) to 2.5805(13) Å for $Ag_2MgSn_3S_8$ (Table 5). Due to the larger ionic radius of Ag^+ with 1.14 Å for a coordination number of four compared to that of Cu^+ with 0.74 Å,[16] the unit cell of $Ag_2MgSn_3S_8$ is larger than that of $Cu_2MgSn_3S_8$.

The unit cells of $Cu_2MgSn_3S_8$ and $Ag_2MgSn_3S_8$ are smaller as compared to those of the corresponding Cd-bearing Cu- and Ag-compounds which can be simply explained by the smaller ionic radii of Mg^{2+} (sixfold coordination) of 0.86 Å compared to that of octahedrally surrounded Cd^{2+} with 1.09 Å.[16] The interatomic distances Cu/Ag–S and (Mg/Sn)–S in $Cu_2MgSn_3S_8$ and $Ag_2MgSn_3S_8$ (Table 5) correlate well with those observed for $Cu_2CdSn_3S_8$ (Cu–S: 2.30(1) Å; [(Cd/Sn)–S: 2.61(2) Å][5] and $Ag_2CdSn_3S_8$ [Ag–S: 2.489(3) Å; (Cd/Sn)–S: 2.602(3) Å][6] with slightly larger Cu- and Ag-centered sulfide tetrahedra and smaller Mg/Sn-centered sulfide octahedra.

In order to give more detailed information on the formation of well-crystalline powders, some details for $Cu_2MgSn_3S_8$ are presented in the following: first of all, it can be seen that the thiospinel was formed during milling (Figure 3). Broadened reflections clearly point to small particle sizes. Consequently, the crystallite sizes of the milled and annealed samples were calculated using the Scherrer equation:[17]

$$\Delta(2\theta) = \kappa\lambda/L\cos\theta_0$$

where $\Delta(2\theta)$ is the full width at half maximum (FWHM), κ is the Scherrer form factor (for this determination a factor of 0.9 was used), λ is the wavelength, L is the mean size of the crystallites, and θ_0 is the diffraction angle. The crystallites after

Table 3. Refined atomic parameters for $Cu_2MgSn_3S_8$ (standard deviations in parenthesis).

Atom	Wyckoff	x	y	z	s.o.f	B_{iso} (Å)^2
Cu	8*a*	1/8	1/8	1/8	1	2.01(3)
Mg	16*d*	1/2	1/2	1/2	0.25	0.46(2)
Sn	16*d*	1/2	1/2	1/2	0.75	0.46(2)
S	32*e*	0.74624(9)	x	x	1	1

Table 4. Refined atomic parameters for $Ag_2MgSn_3S_8$ (standard deviations in parenthesis).

Atom	Wyckoff	x	y	z	s.o.f	B_{iso} (Å)^2
Ag	8*a*	1/8	1/8	1/8	1	1.83(3)
Mg	16*d*	1/2	1/2	1/2	0.25	0.78(4)
Sn	16*d*	1/2	1/2	1/2	0.75	0.78(4)
S	32*e*	0.74097(11)	x	x	1	1

Table 5. Interatomic distances /Å in $Cu_2MgSn_3S_8$ and $Ag_2MgSn_3S_8$ (standard deviations in parenthesis).

$Cu_2MgSn_3S_8$		$Ag_2MgSn_3S_8$	
Cu–S	2.3233(10)	Ag–S	2.4825(13)
(Mg/Sn)–S	2.5658(10)	(Mg/Sn)–S	2.5805(13)

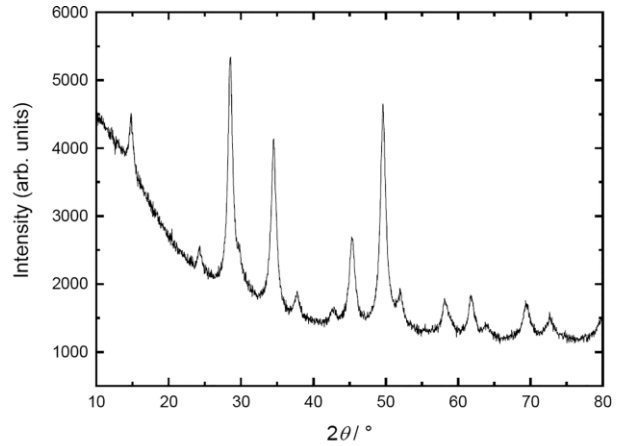

hkl	2θ [°]	Crystallite size after milling [nm]	Crystallite size after annealing [nm]
311	28.5	11.0±0.3	31.8±0.3
400	34.5	9.3±0.4	33.6±0.3
333	45.3	9.3±0.3	35.1±0.3

Figure 3. X-ray diffraction patterns of milled (top) and annealed (middle) $Cu_2MgSn_3S_8$ samples, supplemented by a Table presenting the calculated crystallite sizes for selected reflections.

the milling procedure are rather small (in the range of 9.3 ± 0.4 nm to 11.0 ± 0.3 nm). After the subsequent annealing step, described in the experimental part, the mean crystallite sizes for $Cu_2MgSn_3S_8$ are in the range from 31.8 ± 0.3 nm to 35.1 ± 0.3 nm. In comparison to $Cu_2MgSn_3S_8$, smaller particles were calculated for $Ag_2MgSn_3S_8$ after the milling treatment (in the range of 4.7 ± 0.7 nm to 5.9 ± 0.2 nm) while similar crystallite sizes were observed after the annealing step (in the range of 32.7 ± 0.4 nm to 35.6 ± 0.5 nm).

UV/Vis Spectroscopy

The optical properties of black-colored $Cu_2MgSn_3S_8$ and $Ag_2MgSn_3S_8$ powders were measured in diffuse reflectance geometry. The optical bandgaps were calculated using the Tauc plot method.[18,19] A direct optical bandgap of ca. 1.65 eV was determined for both Mg-containing compounds whereas narrower indirect optical bandgaps of ca. 1.42 eV for $Cu_2MgSn_3S_8$ and ca. 1.40 eV for $Ag_2MgSn_3S_8$ were observed (Figure 4).

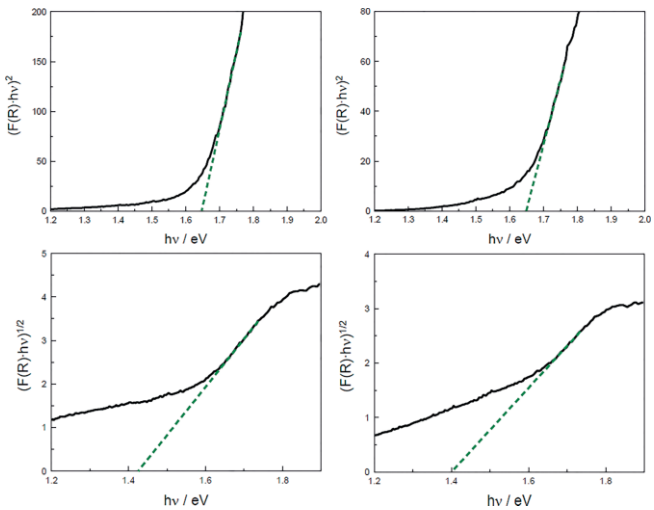

Figure 4. UV/Vis spectra of $Cu_2MgSn_3S_8$ (left) and $Ag_2MgSn_3S_8$ (right) with Tauc plot determination of the direct (top) and indirect (bottom) optical bandgaps.

Magnetic Properties

The temperature dependence of the magnetic susceptibility of the polycrystalline $Cu_2MgSn_3S_8$ sample is presented in Figure 5. Down to about 50 K we observe almost temperature independent behavior. The room temperature value of -150×10^{-6} emu·mol^{-1} indicates diamagnetism, i.e. closed-shell behavior in agreement with the electron-precise description. The increase of the susceptibility towards lower temperature results from small amounts of paramagnetic impurity phases (Curie tail).

Since we deal with an electron-precise compound, one can compare the experimentally determined susceptibilities with

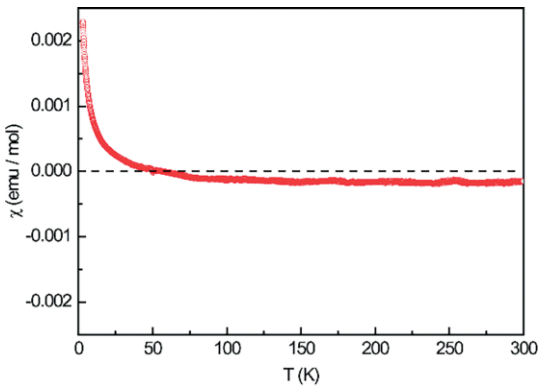

Figure 5. Temperature dependence of the magnetic susceptibility χ of $Cu_2MgSn_3S_8$ measured in ZFC mode with an applied magnetic field strength of 10 kOe.

those calculated from diamagnetic increments.[20] Using the increments (in units of -10^6 emu·mol^{-1}) for Cu^+ (12), Mg^{2+} (5), Sn^{4+} (16) and S^{2-} (30) we obtain a value of -307×10^{-6} emu·mol^{-1} for the intrinsic diamagnetic contribution of $Cu_2MgSn_3S_8$. The experimental value is of the same order of magnitude. Due to the small paramagnetic impurity phase we observe a smaller experimental value.

Mössbauer Spectroscopy

The experimental and simulated ^{119}Sn Mössbauer spectrum of $Cu_2MgSn_3S_8$ (6 K data) is presented in Figure 6. The corresponding fitting parameters are listed in Table 6. The spectrum could reliably be reproduced with a single signal with a small quadrupole splitting contribution, most likely a consequence of the mixed site occupancy on the 16*d* position, generating small distortions. The isomer shift value is in excellent agreement with thiostannates (IV).[21] The slightly enhanced line widths parameter also accounts for domain formation, resulting from the 16*d* mixed occupied site.

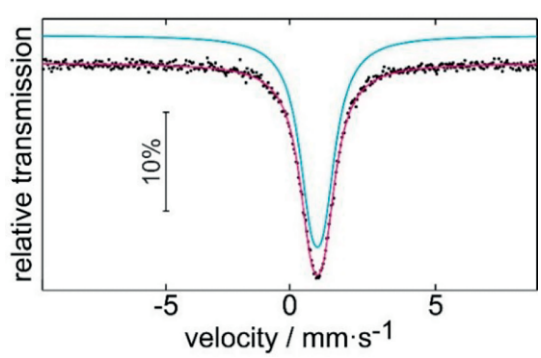

Figure 6. Experimental (black dots) and simulated (red line) ^{119}Sn Mössbauer spectrum of $Cu_2MgSn_3S_8$ at 6 K.

Table 6. Fitting parameters of the ^{119}Sn Mössbauer spectroscopic measurement on $Cu_2MgSn_3S_8$ at 6 K. δ = isomer shift, ΔE_Q = electric quadrupole splitting, Γ = experimental line width.

Compound	δ /mm·s^{-1}	ΔE_Q /mm·s^{-1}	Γ /mm·s^{-1}
$Cu_2MgSn_3S_8$	1.113(3)	0.512(14)	1.254(14)

Conclusions

Two new thiospinels of general formula $A^I_2B^{II}C^{IV}_3S^{VI}_8$ were synthesized via a two step mechanochemical synthesis route. $Cu_2MgSn_3S_8$ and $Ag_2MgSn_3S_8$ were formed after milling in a high energy planetary ball mill. Powders of good crystallinity were obtained after annealing in H_2S-atmosphere at 823 K. X-ray diffraction studies supported by EDX analyses show that phase-pure $Cu_2MgSn_3S_8$ and $Ag_2MgSn_3S_8$ samples have been synthesized. All compounds crystallize in the cubic space group $Fd\bar{3}m$ with a statistical distribution of Mg and Sn at Wyckoff position 16*d*. The direct optical bandgap is determined to ca. 1.65 eV for both compounds. These experiments again show the large potential of mechanochemical routes for synthesizing complex sulfides. Magnetic susceptibility studies and ^{119}Sn Mössbauer spectra manifest the electron-precise description and thiostannate (IV) character.

Experimental Section

Synthesis: The quaternary thiospinels $Cu_2MgSn_3S_8$ and $Ag_2MgSn_3S_8$ were synthesized in a high energy planetary Mono Mill Pulverisette 7 (Fritsch, Idar-Oberstein, Germany) with a subsequent annealing step in a tube furnace. Stoichiometric amounts of the corresponding binary sulfides (Ag_2S (Schuchardt), CuS, MgS, SnS) and sulfur (Fluka, 99.99 %) were filled in a 45 mL zirconia grinding beaker with six zirconia balls and ground at a rotational speed of 450 rpm for four hours. In order to obtain highly crystalline powders, the thiospinels were annealed at 823 K for three hours under flowing H_2S gas after milling. An 0.1 M $Cu(NO_3)_2$ solution and H_2S gas (Air Liquide, 99.5 %) were used for the precipitation of CuS. For MgS, amorphous MgO was prepared by a modified Pechini method[22] followed by sulfidation of the obtained magnesia in H_2S-atmosphere at 1023 K for three hours. SnS was synthesized using a high-temperature solid-state synthesis route based on the elements Sn (Merck, 99.9 %) and S (Fluka, 99.99 %) as starting materials (evacuated and sealed SiO_2-ampoules).

Chemical and Structural Characterization: A Panalytical X'Pert PRO diffractometer with Cu-K_α radiation (Bragg–Brentano geometry) was used for the X-ray diffraction measurements. The diffraction data was obtained over an angular range of 10–120° with a step size of 0.026° and an exposure time of 60 s at each point. Rietveld refinements[23] were carried out using the program Fullprof Suite[24] by applying a pseudo-Voigt function. For elementary analysis, energy dispersive X-ray spectroscopy (EDX) was carried out using a DSM 982 GEMINI spectrometer (Carl Zeiss AG, Oberkochen, Germany) equipped with a XFlash 6|60 detector (Bruker, Billerica, USA). EDX measurements were performed at the Zentrum für Elektronenmikroskopie (ZELMI) of TU Berlin. For the determination of the phase composition using EDX analysis a device error of 5 % is presumed. Furthermore, the sulfur content of both samples was determined using a FlashEA 1112 elemental analyzer (Thermo Scientific™, Waltham, USA) with a given device error of about 2 %. Additional measurements were carried out with a RIGAKU SmartLab 3 kW system equipped with a Kα_1 unit (Johansson-type Ge crystal, Cu-$K_{\alpha1}$ radiation, λ = 1.54060 Å).

Further details of the crystal structure investigations may be obtained from the Fachinformationszentrum Karlsruhe, 76344 Eggenstein-Leopoldshafen, Germany (Fax: +49-7247-808-666; E-Mail: crysdata@fiz-karlsruhe.de, http://www.fiz-karlsruhe.de/request for deposited data.html) on quoting the depository numbers CSD-1946219 and CSD-1946220.

UV/Vis Measurements: UV/Vis measurements in diffuse reflectance mode were performed using an Evolution 220 UV/Vis spectrometer (Thermo Scientific™, Waltham, USA) equipped with a Xenon Flash lamp and a dual silicon photodiode detector. The obtained spectra were converted by the Kubelka-Munk function to absorption spectra, the optical bandgaps were determined using the Tauc plot method.[18,19] The standard deviation for E_g was estimated close to ± 0.5 eV.

Magnetic Properties: $Cu_2MgSn_3S_8$ was used as a polycrystalline powder, packed in a PE capsule and attached to the sample holder rod of a Vibrating Sample Magnetometer unit (VSM) for measuring the magnetization M(T,H) in a Quantum Design Physical-Property-Measurement-System (PPMS). The sample was investigated in the temperature range of 2.5–300 K with an applied external magnetic field of 10 kOe.

Mössbauer Spectroscopy: A $Ca^{119m}SnO_3$ source was used for the ^{119}Sn Mössbauer spectroscopic investigation. The sample was placed within a thin-walled PMMA container. A palladium foil of 0.05 mm thickness was used to reduce the tin K X-rays concurrently emitted by this source. The measurement was conducted in a continuous flow cryostat system (Janis Research Co LLC) at 6 K. The spectrum was fitted with the Normos-90 software package.[25]

Acknowledgements

This work was supported by the Deutsche Forschungsgemeinschaft (LE 781/19-1). Special thanks to the Zentrum für Elektronemikroskopie (ZELMI) of the TU Berlin giving access to EDX measurements. All EDX measurements were carried out by *Dr. Stefan Berendts* (TU Berlin). Combustion analysis were performed by *Juana Krone* (TU Berlin).

Keywords: Mechanochemical synthesis; Planetary ball mill; Thiospinels; Rietveld refinement; Magnetic properties

References

[1] J. C. Jumas, E. Philippot, M. Maurin, *Acta Crystallogr. Sect. B* **1979**, *35*, 2195–2197.
[2] P. Lavela, J. L. Tirado, J. Morales, J. Olivier-Fourcade, J. C. Jumas, *J. Mater. Chem.* **1996**, *6*, 41–47.
[3] G. Garg, S. Bobev, A. K. Ganguli, *J. Alloys Compd.* **2001**, *327*, 113–115.
[4] G. Garg, K. V. Ramanujachary, S. E. Lofland, M. V. Lobanov, M. Greenblatt, T. Maddanimath, K. Vijayamohanan, A. K. Ganguli, *J. Solid State Chem.* **2003**, *174*, 229–232.
[5] S. I. Chykhrij, L. V. Sysa, O. V. Parasyuk, L. V. Piskach, *J. Alloys Compd.* **2000**, *307*, 124–126.
[6] O. V. Parasyuk, I. D. Olekseyuk, L. V. Piskach, S. V. Volkov, V. I. Pekhnyo, *J. Alloys Compd.* **2005**, *399*, 173–177.
[7] M. A. Cochez, J. C. Jumas, P. Lavela, J. Morales, J. Olivier-Fourcade, J. L. Tirado, *J. Power Sources* **1996**, *62*, 101–105.
[8] J. Yajima, E. Ohta, Y. Kanazawa, *Mineral. J.* **1991**, *15*, 222–232.
[9] C. Branci, M. Womes, P. E. Lippens, J. Olivier-Fourcade, J. C. Jumas, *J. Solid State Chem.* **2000**, *150*, 363–370.
[10] V. P. Sachanyuk, A. O. Fedorchuk, I. D. Olekseyuk, O. V. Parasyuk, *Mater. Res. Bull.* **2007**, *42*, 143–148.
[11] Z. Kormosh, A. Fedorchuk, K. Wojciechowski, N. Tataryn, O. Parasyuk, *Mater. Sci. Eng. C* **2011**, *31*, 540–544.
[12] C. Branci, J. Sarradin, J. Olivier-Fourcade, J. C. Jumas, *J. Power Sources* **1999**, *81–82*, 282–285.
[13] G. Garg, S. Bobev, A. Roy, J. Ghose, D. Das, A. K. Ganguli, *Mater. Res. Bull.* **2001**, *36*, 2429–2435.
[14] G. Garg, S. Bobev, A. K. Ganguli, *Solid State Ion.* **2002**, *146*, 195–198.
[15] O. V. Krykhovets, L. V. Sysa, I. D. Olekseyuk, T. Glowyak, *J. Alloys Compd.* **1999**, *287*, 181–184.
[16] R. D. Shannon, *Acta Crystallogr., Sect. A* **1976**, *32*, 751–767.
[17] P. Debye, P. Scherrer, *Nachrichten von der Gesellschaft der Wissenschaften zu Göttingen, Mathematisch-Physikalische Klasse* **1918**, 101–120.
[18] J. Tauc, R. Grigorovici, A. Vancu, *Phys. Status Solidi B* **1966**, *15*, 627–637.
[19] J. Tauc, *Mater. Res. Bull.* **1968**, *3*, 37–46.
[20] G. A. Bain, J. F. Berry, *J. Chem. Educ.* **2008**, *85*, 532–536.
[21] P. E. Lippens, *Phys. Rev. B* **1999**, *60*, 4576–4586.
[22] M. P. Pechini. *US Patent No. 3330697* **1967**.
[23] H. M. Rietveld, *J. Appl. Crystallogr.* **1969**, *2*, 65–71.
[24] J. Rodriguez-Carvajal. Abstracts of the Satellite Meeting on Powder Diffraction of the XV. Congress of the IUCr **1990**, 127.
[25] R. A. Brand. WINNORMOS for IGOR6, version for IGOR 6.2 or above: 22.02.2017, Universität Duisburg, Duisburg, Germany **2017**.

Received: August 12, 2019
Published Online: January 3, 2020